

Strain controlled medium cycle fatigue of a notched Pb-Sn-Cd lead alloy

Luigi M. Viespoli¹, Audun Johanson², Antonio Alvaro³, Bård Nyhus³, Filippo Berto¹

¹*Department of Mechanical and Industrial Engineering, Norwegian University of Science and Technology (NTNU), Norway*

²*Nexans Norway, Innspurten 9, 0663 Oslo, Norway*

³*Sintef Industry, Richard Birkelands vei 2B, 7031, Trondheim, NORWAY*

luigi.m.viespoli@ntnu.no

[+47 459 13 281](tel:+4745913281)

Richard Birkelands vei 2B, Trondheim, Norway

Abstract: During the extrusion process of subsea power cable sheathing layer it is possible that metallic and/or non-metallic debris present in the processing environment enter the metal lattice originating discontinuities that might have a detrimental effect on the fatigue life and the overall integrity of the sheathing. In order to understand the influence of these production defects on the reliability of installed power-lines, a series of specimens directly retrieved from the extruded sheathing were fatigue tested at different strain rates and range both in presence and absence of a non-passing through notch simulating the geometrical discontinuity induced by a particle. In order to collect the necessary information for the understanding of the failure mechanism, Digital Image Correlation and Scanning Electron Microscopy were used to understand the influence of the testing condition on the material resistance and failure mode.

Keywords: Lead, creep-fatigue interaction, digital image correlation, notch sensitivity

Introduction

To prevent the failure of power lines for electric short circuit it is necessary to impede the penetration of water through the polymer wall. This is achieved by the addition of a layer of stable metal such as lead. The technology used for such application is not recent, but most of the studies performed are dated and many issues regarding the topic are still unclear, while the

production of power cables greatly relies on previous experience. In the case of the alloy object of the study, which has a melting temperature of 590 K, operational temperature (i.e. room temperature) above its recrystallization temperature, time dependent plasticity phenomena must be taken into account [1] to provide a reliable prediction of the mechanical response of the material. The mechanisms of creep deformation of lead alloys were investigated by Feltham [2] with focus on the effect of the inter-granular substructure and grain size. A qualitative classification of fitness for different kind of power cable application was performed by Harvard [3]. An investigation on the compressive creep behavior of cable sheathing and the influence of alloy elements has been performed by Sahota et al. [4]. Dollins and Betzer [5] studied the influence of the production variables on the long term plasticity and fatigue behavior of lead alloys. Anelli et al. [6] found a non-significant influence of grain size and temperature on the fatigue life of cable sheathing lead alloys E and Pb-Sb. Analyzing the behavior of the cable sheathing as a creep problem, several effects have to be considered. For the application of lead and lead-free solders, a variation of the apparent elastic modulus was detected in function of the temperature and strain rate which the material is subjected to [7,8,9]. Grain boundary sliding has a consistent contribution on the creep deformation of polycrystalline commercially pure metals [10, 11], leading to greater deformation in the presence of smaller grains. The influence of creep and microstructure on the tensile properties of a PbSnSb alloy used for the manufacturing of subsea power cables was investigated by Viespoli et al. [12] finding a correlation between the grain size and the stress level reached for a given strain rate. Johanson et al. [13] tested a batch of notched and un-notched lead fatigue specimens at two different strain levels and testing frequencies. The influence of sharp and blunt V-notches and semi-circular notches on the medium cycle fatigue, in the case of an aluminum alloy, was studied by Negru et al. [14]. With regards to the tests in [13], although the finite element modelling shows a significant increment of the strain range due to the notch, this was not determinant for the failure mechanism. In the present work, these results are recalled and integrated with new elements to enhance the understanding of the material behavior. The material plastic response of the same alloy was obtained by performing tensile testing on flat dog-bone samples and extracting the strains by digital image correlation (DIC) post-processing. A second batch of four new fatigue tests was performed at two different strain rates and one strain range. These tests were recorded by a digital camera at selected intervals in order to reconstruct the strain pattern on the specimen's surface by DIC post-processing. The effective Von Mises strain range has been extracted from the crack initiation locations and correlated to the crack initiation

number of cycles. The fracture surfaces were investigated by the use of a scanning electron microscope (SEM) to understand the damage progression mechanics.

Material and samples

In the manufacturing of lead sheaths for power cables, the unwanted presence of hard particles included in the material due to the production process may occur as showed in Figure 1. It is then important to understand the influence of these hard particles, which create a discontinuity in the material and intensify the strain field, on the overall fatigue life. The geometry of the notches to be introduced in the samples was decided from the observation of real defects on sheathing samples and machined by electro discharge machine (EDM). The procedure adopted was to simulate the presence of the defect machining a small blind hole, acting as a notch, on the convex surface of the specimen. The effect of the discontinuity was investigated testing both notched and un-notched samples at the frequencies of 5 and 10 Hz for two strain ranges, 0.15 and 0.28%. The cable sheathing was extruded from material according to PB012K in EN 12548. The main alloying elements are tin (Sn) and cadmium (Cd). Minor additions of tellurium (Te) for grain stabilization are also present. The chemical composition, measured by optical emission spectroscopy on the extrusion material, is reported in Table 1. The test specimens were machined according to the specifications in Figure 2 from 80 mm nominal diameter tubes. The curvature in the transversal section was kept in order to prevent buckling in the compressive phase and limit the work hardening during the production of the sample.

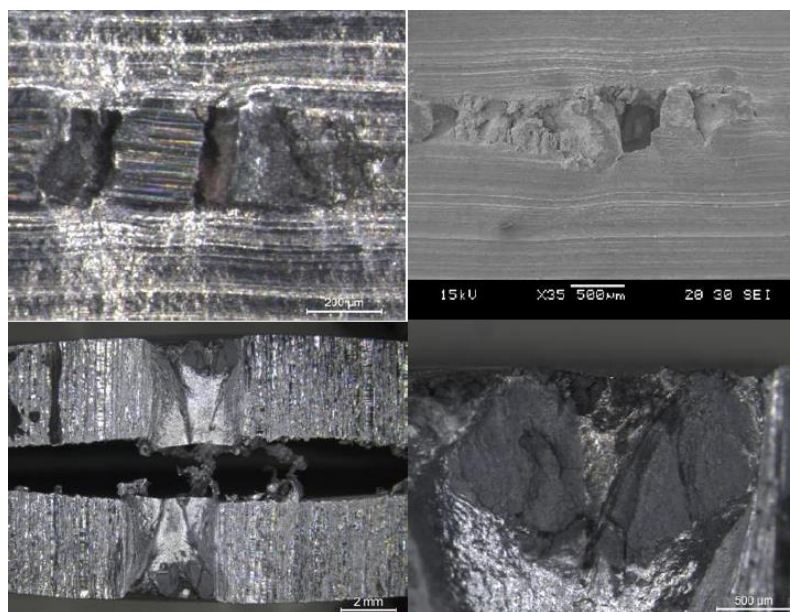


Figure 1. Magnifications of defects created in the extruding process.

Element	Sn	Te	Cd
Weight %	0.175-0.225	0.0008-0.0025	0.60-0.90

Table 1. Chemical composition of lead alloy 1/2C+Te.

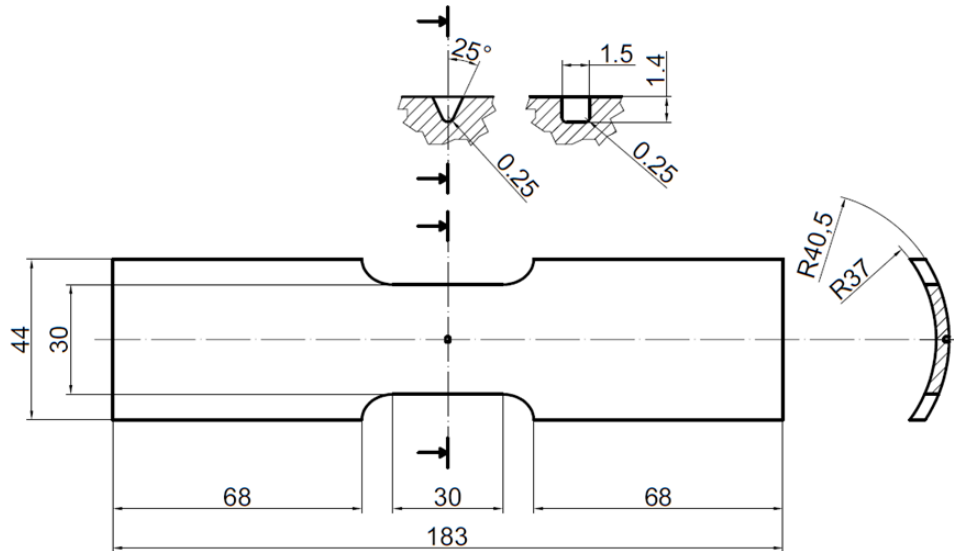


Figure 2. Nominal dimensions of the specimens and of the notch practiced.

Material tensile characterization

In order to have an estimate of the strain rate sensitivity in the chosen strain ranges, tensile testing at two different strain rates, $1E-2$ and $1E-3$ s⁻¹, was performed. The tensile testing was executed on flat dog-bone samples, see Figure 3. The strains were obtained through DIC post-processing. The mechanical response of the material treated is strongly influenced by time dependent phenomena [12], thus it was necessary to perform a tensile characterization at two different strain rates in the range of the fatigue testing, but also compatible with the capabilities of the equipment. The fatigue testing was executed at two different strain ranges and two frequencies, as indicated in Table 2. The value indicated in Table 2 as nominal strain rate is the averaged strain rate value calculated considering a constant strain rate development through the whole cycle even if the imposed load cycle was of sinusoidal shape. Even if the testing conditions have a nominal strain rate 1.5 to 3 times greater than the highest adopted in the tensile testing, figure 4 shows the reduced influence of time dependent deformation in the strain rate range of interest. In fact, the two tensile curves obtained at $1E-2$ and $1E-3$ s⁻¹ are mostly correspondent.

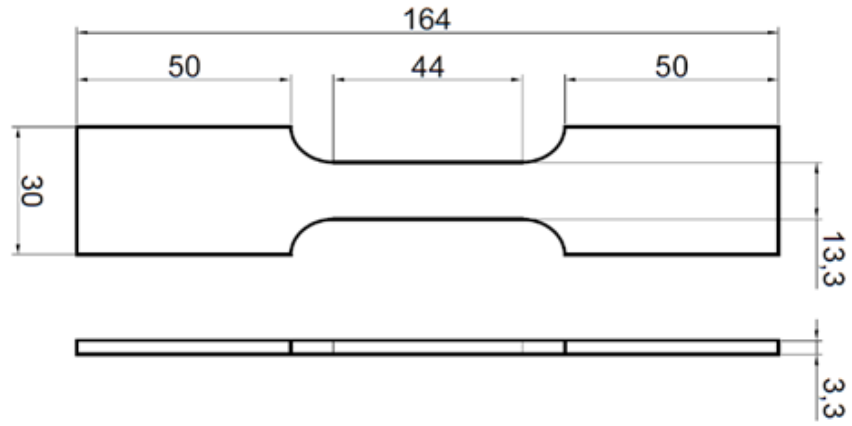


Figure 3. Geometry of the tensile specimens for material calibration.

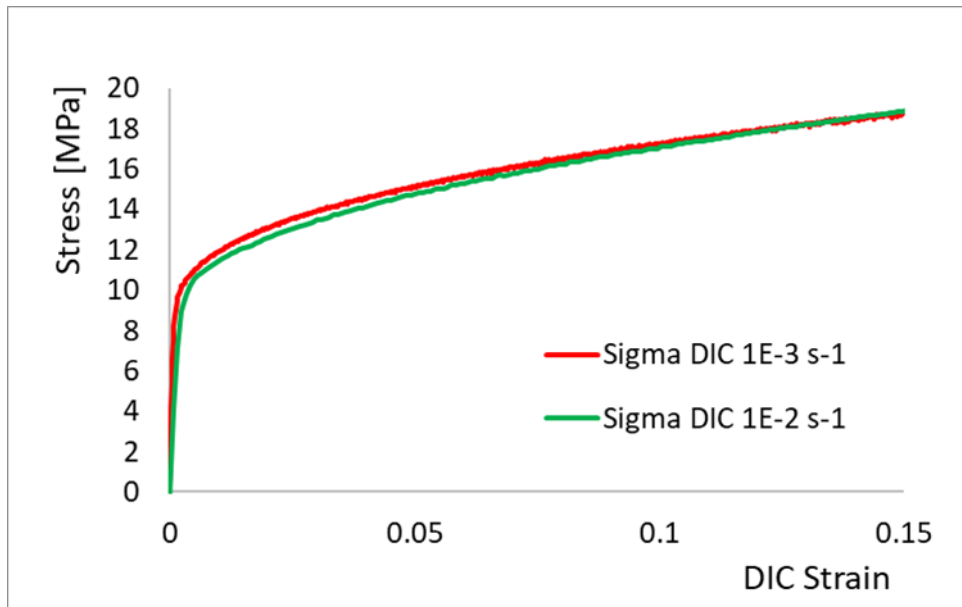


Figure 4. Tensile testing characterization.

Strain Range [%]	Load Ratio R	Frequency [Hz]	Nominal Strain Rate [s-1]
0.28	-1	5	2.8E-2
0.15	-1	5	1.5E-2
0.15	-1	10	3E-2

Table 2. Nominal fatigue testing conditions.

Fatigue testing

The fatigue testing was run in position control according to the conditions reported in Table 2, that is frequencies of 5 and 10 Hz and nominal strain ranges of 0.15 and 0.28 %. The load ratio adopted was equal to -1 in terms of displacement. Two different series of testing were executed, the second of which with the use of digital image correlation. In the first batch, nineteen specimens were tested without DIC [13]. The following procedure was adopted to determine the test parameters: an extensometer was used during the first upload phase to register the necessary machine displacement to be imposed as the cycle amplitude. The extensometer was then removed and, before the test was initiated, the marks left by the extensometer clips were removed by careful manual grinding to prevent early crack initiation. The results of the fatigue testing of this first batch are summarized in figure 6. At the highest strain range and lowest frequency, no influence of the presence of the notch was detected in terms of cycles to failure. For all the specimens the failures have started from the edge and propagated towards the middle of the specimen, passing through the notch in case of the notched ones. Stronger influence was observed for the tests at the lower strain range: both at 5 and 10 Hz, the notched samples had a shorter fatigue life than the respective un-notched. In addition the cracks were seemingly more randomly positioned: they did not start from the notch, but from the edges of the specimens, at the fillet radius or at the height of the notch, without a significant correlation with the presence of the discontinuity, see Figure 5.

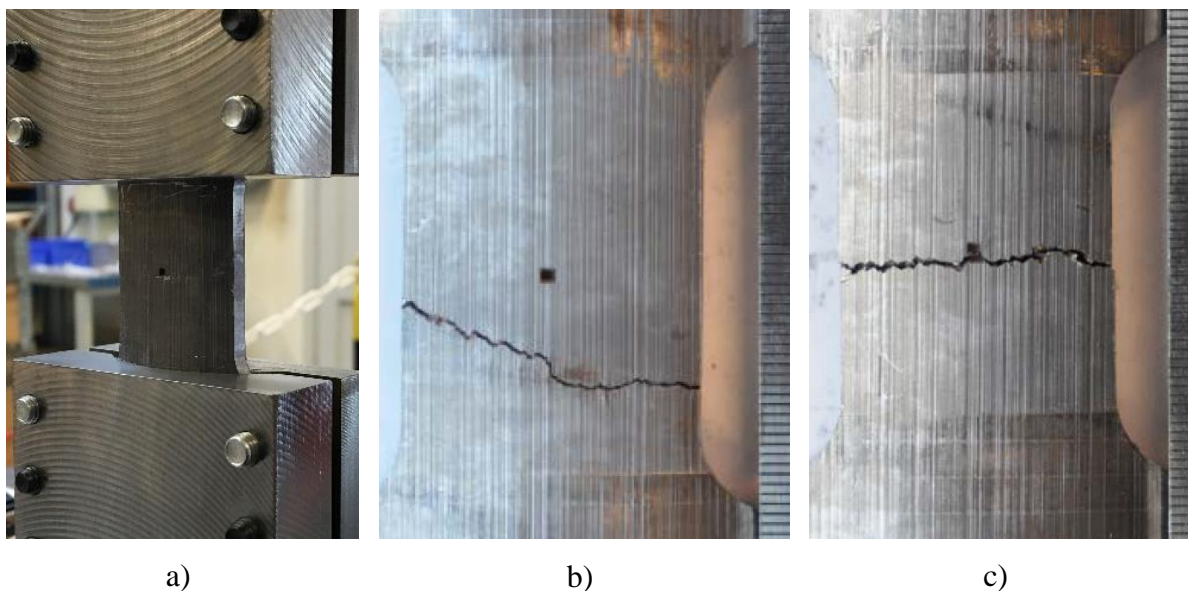


Figure 5. The pictures show the sample in the custom-made, curved clamping system (a), two different crack paths on notched samples (b, c).

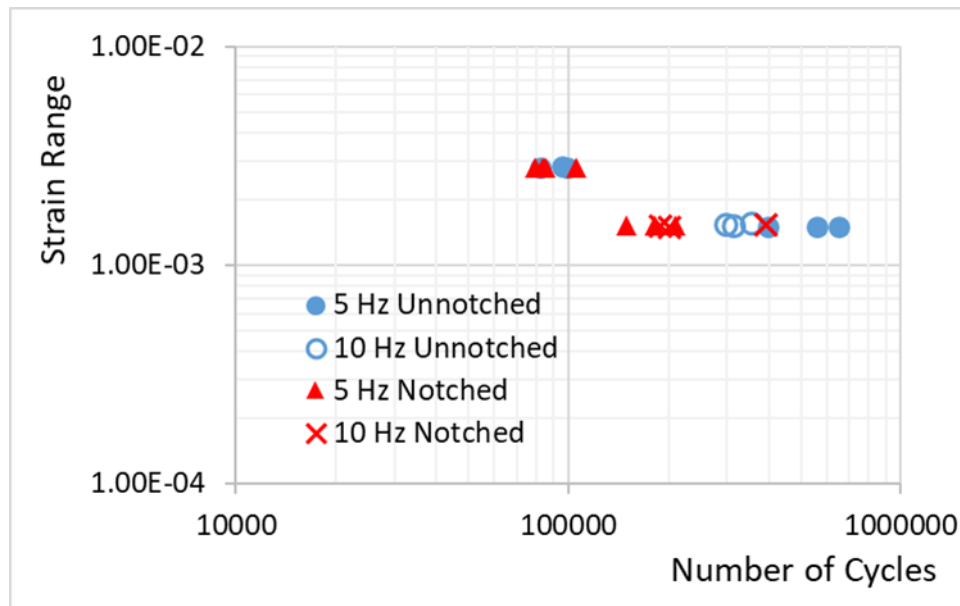


Figure 6. Summary of the fatigue testing results obtained by Johanson et al. [13]. Number of cycles to resistance drop to 200 N in the tensile phase of the cycle.

DIC Strain-Life results synthesis

The second batch of fatigue tests was performed at 5 and 10 Hz at a nominal strain range of 0.15 % following the same procedure and adopting the same equipment used for the first batch and having one notched sample for each testing frequency. In addition, these tests were recorded by a Prosilica GC 2450 digital camera to reconstruct the strain field on the specimens' convex surfaces by DIC post-processing, executed with the software eCorr. Being the acquisition rate of the camera limited to 10 Hz and due to limitations of the DIC software, it was not possible to either reconstruct the strain evolution within one single cycle or to record the points of maximum positive and negative strain. Therefore an acquisition period slightly longer than the fatigue cycle period was adopted and an equivalent strain cycle in DIC was obtained out of 40 real fatigue cycles: one image for each real cycle, but each at a higher angular position than in the previous one. Due to the huge amount of data the images were not captured during the whole test, but only at selected intervals. Following this procedure it was possible to compute the strain range in selected areas on the specimen's surface and adopt it as failure parameter. The crack initiation has been observed by means of visual imaging. The first initiation phase however has not been detected due to the discrete acquisition time frame during the tests. On the other hand it was possible to observe the moment before and after the onset of the crack growth. This has allowed to define, at least, an upper and lower threshold for crack

initiation. The effective von Mises strain range was computed by the DIC post-processor and correlated to the crack initiation upper and lower threshold. These values were extracted from the crack initiation sites, Figure 7, and plotted in Figure 8. The software eCorr allows to directly compute the equivalent von Mises strain at the surface of the material, that is:

$$\varepsilon_{eff} = \sqrt{\frac{2}{3}(\varepsilon_1^2 + \varepsilon_2^2 + \varepsilon_3^2)} \quad (1)$$

In order to execute this calculus it is necessary to have an approximation of the third principal strain. Assuming negligible elastic strains and incompressible plasticity, approximation feasible due to the highly plastic behavior of the alloy, this is equal to:

$$\varepsilon_3 = -(\varepsilon_1 + \varepsilon_2) \quad (2)$$

Equations 1 and 2 are reported from the software theory guide [15]. The values obtained following the described procedure on the second batch, Figure 8, are in line with the results obtained from the first batch, Figure 6, being slightly more conservative. In this case, contrarily to what had happened for the samples in the first batch, the notched sample tested at a frequency of 10 Hz presented cracks originating also from the notch, while the specimen tested at a frequency of 5 Hz did not present any cracking at the notch. The different behavior could be due to an enhanced notch sensitivity of the material at higher strain rates, but other cracks were contemporarily generated also from other areas of the same sample subjected to a much smaller theoretical stress concentration factor, i.e. the fillet radius.

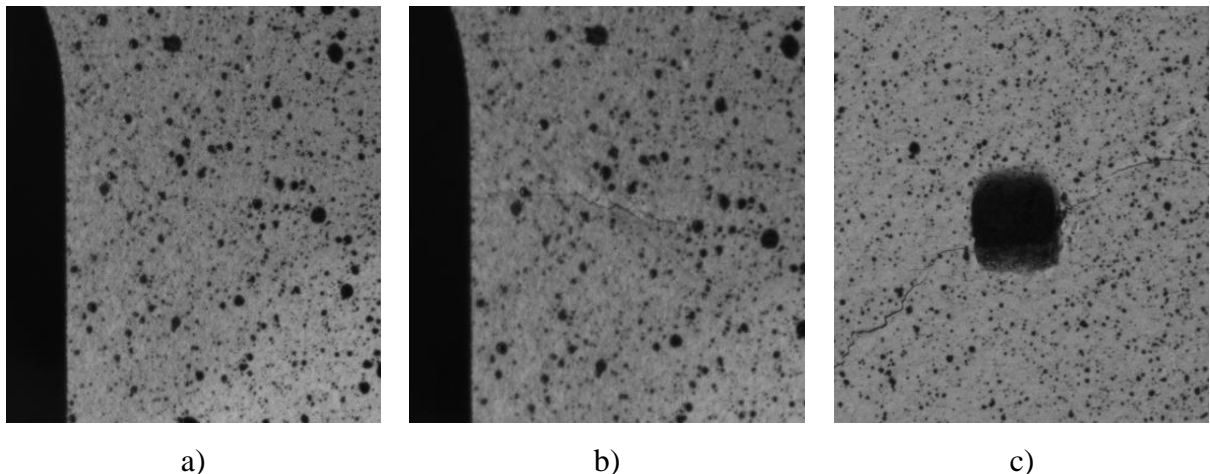


Figure 7. DIC images of a sample before (a) and after (b) crack initiation in the proximity of the fillet radius. Cracks developing from the notch (c).

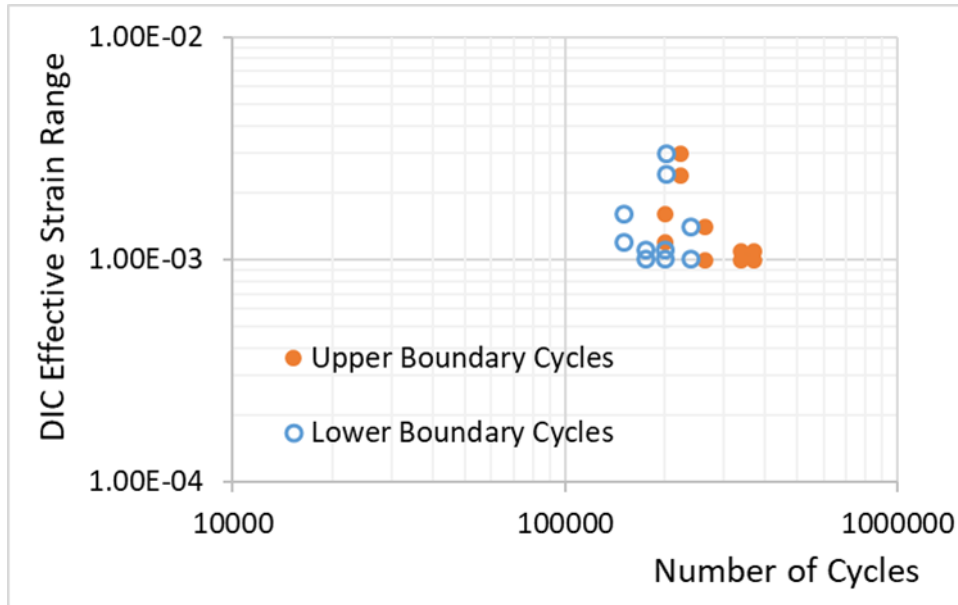


Figure 8. Summary of the strain range detected by DIC in the crack initiation sites. The number of cycles is to crack initiation and the lower and upper boundary cycles are the cycles of the DIC window immediately before and after the crack initiation.

Second batch failure analysis

The fracture surfaces of the samples tested in the second batch and recorded for DIC post-processing, were investigated in a scanning electron microscope. Figure 9 shows the crack initiation and propagation from the specimen surface orthogonal to the radial direction, being the radial direction the direction from the curvature axis of the specimen to the specimen's surface, while figure 10 shows the grain de-cohesion caused by the final plastic tearing. Although not clear from the SEM images, the cracks have propagated through the thickness of the specimen along a plane with an inclination of approximately 45° from the loading direction, so in the maximum shear plane, Figure 11. From this observation is deduced that the crack propagation in an alloy characterized by the described elastic-plastic properties in the case of fully reversed loading strongly depends on mode II propagation, in contrast with the effect that a similar load has on an alloy for which the assumptions of linear elastic fracture mechanics are valid, for which the crack propagation is mode I dominated. Figures 12 and 13 show the striations left on the fracture surface during the crack propagation and after the final plastic failure. In particular several secondary cracks are visible. In fact, what was observed in the failed specimens was not a single catastrophic crack, but rather a diffused damage interesting several areas in which the cohesion between the grains is diminished, due to the influence of creep damage on the failure mechanism. The observation of the pronounced strain-rate

sensitivity on the tensile behavior of the alloy, the kind of fatigue damage produced and the differentiation of the fatigue life obtained by a change of the testing frequency, particularly in the case of the un-notched samples tested at a nominal strain range of 0.15 %, indicate that the material is subjected to creep-fatigue interaction damage.

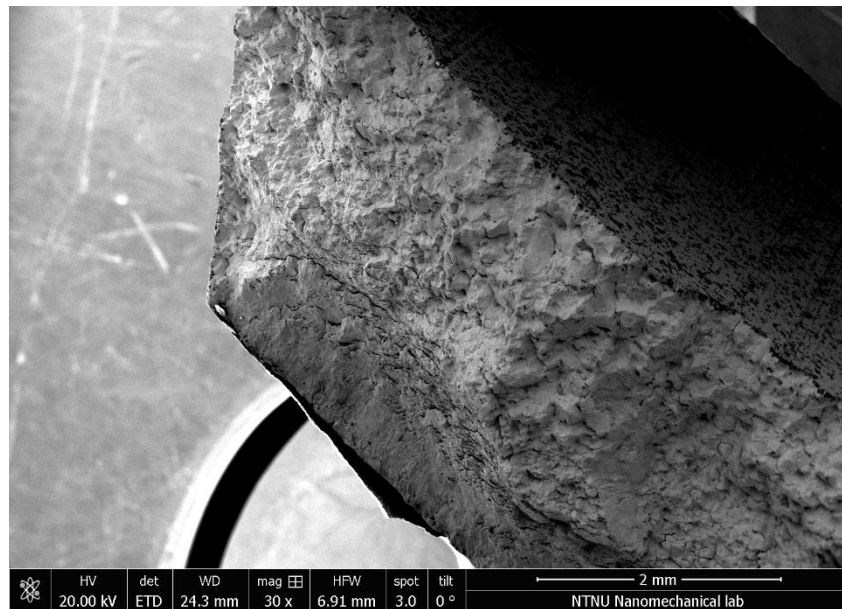


Figure 9. Crack initiation, propagation and plastic fracture on a specimen tested at 5 Hz and at a strain range of 0.15 %.

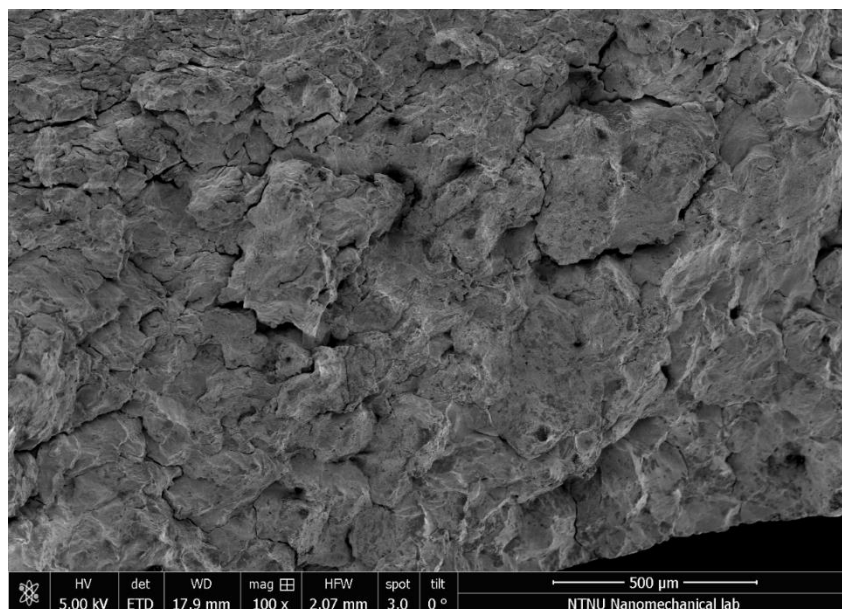


Figure 10. Grain de-cohesion at the final plastic fracture on a specimen tested at 10 Hz and at a strain range of 0.15 %. The fracture location both for the present figure and for the previous fig. 9 is analogous to the one presented in fig. 7b.



Figure 11. Side view of a failed specimen. The shear crack propagation, the multitude of diffused secondary cracks and the final plastic tearing executed at the end of the test are distinguishable.

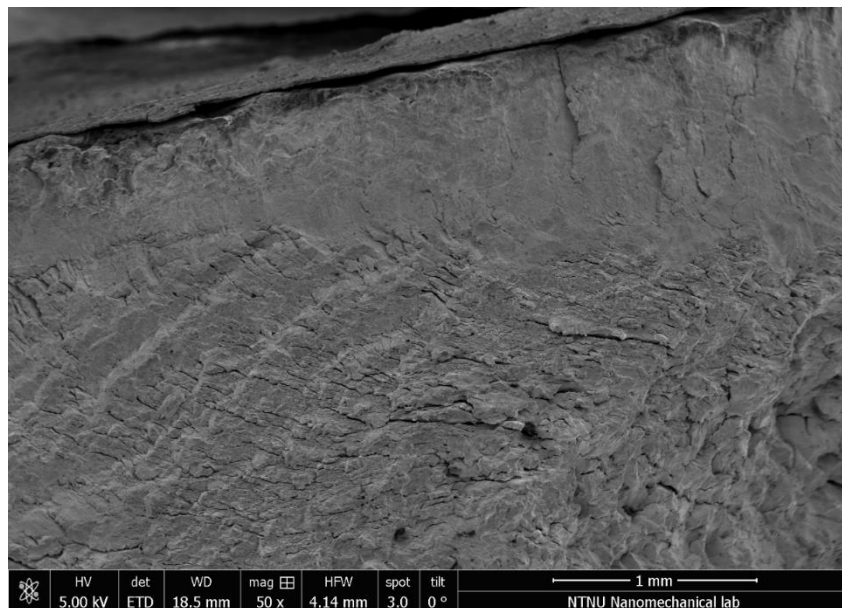


Figure 12. Crack initiation and propagation on a specimen tested at 10 Hz and at a strain range of 0.15 %. On the upper surface, the layer of paint for DIC can be seen.

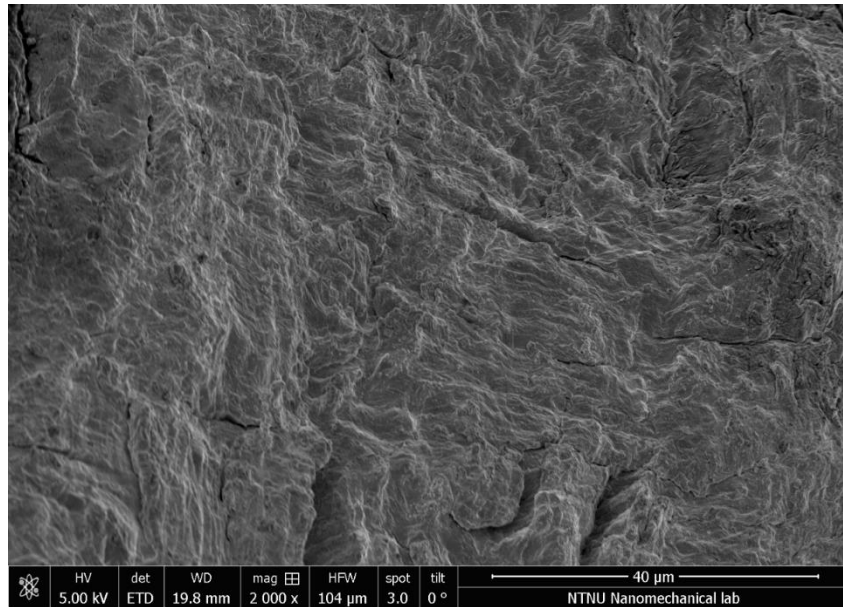


Figure 13. Crack propagation striations on a specimen tested at 10 Hz and at a strain range of 0.15 %. Secondary cracking can be observed.

Conclusions

The present work summarizes the results of static and fatigue testing performed on a number of Pb-Sn-Cd lead alloy specimen, material used in the production of sub-sea power-cable sheathing. The testing was performed in displacement control at two strain ranges and two frequencies. Due to the presence of defects in the components after the extrusion process, a blind notch was machined in part of the specimens. Some of the tests have been recorded by a digital camera for obtaining an approximation of the real strain field with DIC post-processing. The fractures of these samples were then investigated in SEM. The results obtained demonstrate how the highly plastic behavior of the alloy tested yields to a minimal notch sensitivity, with fatigue cracks starting from other location at a much inferior geometrical stress concentration factor. That is, the presence of small defects in the cable sheathing, although to be avoided, does not constitute a high threat to the structural integrity of the same. The propagation of the fatigue cracks at an angle of 45° from the loading direction, that is along the maximum shear plane, means that the propagation of a fatigue crack in a plastic material in fully reversed load is strongly influenced by mode II fracture propagation.

Acknowledgements: The present work was financed by Nexans Norway AS and the Research Council of Norway (IPN in ENERGIX Project number 256367) and performed within the project: Next-generation damage based fatigue of cable sheathing (REFACE).

References

- [1] M.E. Kassner. *Fundamentals of Creep in Materials (Third Edition)*. Butterworth-Heinemann, ISBN 9780080994277. 2015.
- [2] P. Feltham. On the Mechanism of High-Temperature Creep in Metals with Special Reference to Polycrystalline Lead. *Proc Phys Soc.* 69,12-B. 1956.
- [3] D.G. Harvard. *Fatigue of Lead Cable-Sheathing Alloys*. Ontario Hydro research. 1972.
- [4] M.K. Sahota, J.R. Riddington. Compressive creep properties of lead alloys. *Materials and Design.* 21: 159-167. 2000.
- [5] C.W. Dollins, C.E. Betzer. Creep Fracture and Bending of Lead and Lead Alloy Cable Sheathing. *Engineering experiment station bulletin* 440. 1956.
- [6] P. Anelli, F. Donazzi, W.G. Lawson. The fatigue life of lead alloy E as a sheathing material for submarine power cables. *Societa' cavi Pirelli*, pp. 86 SM 393-3. 1986.
- [7] H.L.J. Pang, Y.P. Wang, X.Q. Shi and Z.P. Wang. Sensitivity study of temperature and strain rate dependent properties on solder joint fatigue life. *Proceedings of 2nd Electronics Packaging Technology Conference (Cat. No.98EX235)*, pp. 184-189. 1998.
- [8] P. Lall, D. Zhang, V. Yadav, D. Locker. High Strain-Rate Constitutive Behavior of SACI05 and SAC305 Lead-free Solder. *IEEE*. 2015.
- [9] M. Motalab, Z. Cai, J.C. Suhling, P. Lall, Determination of Anand constants for SAC solders using stress-strain or creep data. *13th InterSociety Conference on Thermal and Thermomechanical Phenomena in Electronic Systems, San Diego, CA*, pp. 910. 2012.
- [10] A. Farghalli, Mohamed, Terence G. Langdon. The transition from dislocation climb to viscous glide in creep of solid solution alloys. *Acta Metallurgica*, Volume 22, Issue 6, pp. 779-788, ISSN 0001-6160. 1974.
- [11] M.E. Kassner. *Five-power-law creep in single phase metals and alloys*. Oxford: Pergamon. 2000.
- [12] L.M. Viespoli, A. Johanson, A. Alvaro, B. Nyhus, A. Sommacal, F. Berto. Tensile characterization of a lead alloy: creep induced strain rate sensitivity. *Materials Science and Engineering: A*, Volume 744, pp. 365-375. 2019.

[13] A. Johanson, L.M. Viespoli, B. Nyhus, A. Alvaro, F. Berto. Experimental and numerical investigation of strain distribution of notched lead fatigue test specimen. MATEC Web Conf. 165 05003. 2018.

[14] R. Negru, D.A. Şerban, L. Marşavina, A. Magda. Lifetime prediction in medium-cycle fatigue regime of notched specimens. Theoretical and Applied Fracture Mechanics. Volume 84, Pages 140-148. 2016.

[15] <http://folk.ntnu.no/egilf/ecorr/doc/definitions/strain/logstrains.html>